

## Structure/Function Analysis of the *Saccharomyces cerevisiae* Trf4/Pol $\sigma$ DNA Polymerase

Zhenghe Wang,<sup>1</sup> Irene B. Castaño,<sup>2</sup> Carrie Adams, Clemence Vu, David Fitzhugh and Michael F. Christman<sup>3</sup>

Department of Microbiology, University of Virginia, Charlottesville, Virginia 22908

Manuscript received April 20, 2001

Accepted for publication October 9, 2001

### ABSTRACT

The Trf4p/Pol  $\sigma$  DNA polymerase (formerly Trf4p/Pol  $\kappa$ ) couples DNA replication to the establishment of sister chromatid cohesion. The polymerase is encoded by two redundant homologs in *Saccharomyces cerevisiae*, *TRF4* and *TRF5*, that together define a fourth essential nuclear DNA polymerase in yeast and probably in all eukaryotes. Here we present a thorough genetic analysis of the founding member of this novel family of DNA polymerases, *TRF4*. Analyses of mutants carrying 1 of 34 "surface-targeted" alanine scanning mutations in *TRF4* have identified those regions required for Pol  $\sigma$ 's essential function, for its role in DNA double-strand break repair, and for its association with chromosomes. The data strongly support the importance of the regions of predicted structural similarity with the Pol  $\beta$  superfamily as critical for Trf4p/Pol  $\sigma$ 's essential and repair functions. Surprisingly, five lethal mutations lie outside all polymerase homology in a C-terminal region. The protein possesses Mg<sup>2+</sup>-dependent 3' to 5' exonuclease activity. Cell cycle analysis reveals that Trf4p/Pol  $\sigma$  associates with chromosomes in G1, S, and G2 phases, but that association is abolished coincident with dissolution of cohesion at the metaphase-to-anaphase transition.

**I**n eukaryotes, sister chromatids are held together during or shortly after their formation until they separate into mother and daughter cells during anaphase. Sister chromatid cohesion is established coincident with DNA replication (UHLMANN and NASMYTH 1998) in a process that requires Eco1p (Ctf7p) and Scc1p (Mcd1p; SKIBBENS *et al.* 1999; TOTH *et al.* 1999). Loading of cohesins onto chromosomes occurs in late G1 (CIOSK *et al.* 2000), meaning that as replication forks move along chromosomes they will encounter cohesin complexes. We have shown that a novel DNA polymerase, Pol  $\sigma$ , is necessary to establish cohesion during S phase (Z. WANG *et al.* 2000; CARSON and CHRISTMAN 2001). Thus, Pol  $\sigma$  may directly couple replication to the action of cohesion factors at replication forks (TAKAHASHI and YANAGIDA 2000). We have proposed a polymerase switch model for cohesion establishment in which Pol  $\sigma$  replaces replicative polymerases upon encounter of the fork with a pre-cohesion site (Z. WANG *et al.* 2000; CARSON and CHRISTMAN 2001). Polymerase switching from Pol  $\alpha$  to Pol  $\delta$  on Okazaki fragments is thought to be accomplished by the replication factor C (RFC) complex (WAGA and STILLMAN 1994). Recent data indicate that

a modified RFC complex, in which CTF18 replaces RFC1, is required for cohesion (HANNA *et al.* 2001), lending strong support to the model.

*TRF4*/Pol  $\sigma$  is conserved in all eukaryotes and we have shown that the human enzyme possesses DNA polymerase activity *in vitro* (Z. WANG and M. F. CHRISTMAN, unpublished observation). Pol  $\sigma$  represents the fourth essential nuclear DNA polymerase, in addition to Pol  $\alpha$ , Pol  $\delta$ , and Pol  $\epsilon$ , in yeast and probably in all eukaryotes. While mutation of both *TRF4* and *TRF5* is lethal in *Saccharomyces cerevisiae* (CASTAÑO *et al.* 1996), a *trf4* single mutant displays a defect in DNA repair (WALOWSKY *et al.* 1999). The relationship of the repair function of *TRF4* to its essential function is unknown at present. A *Schizosaccharomyces pombe* homolog, *cid1*, appears to play a role in the S-phase checkpoint (S. W. WANG *et al.* 2000).

Analysis of the highly conserved *TRF4* gene family has led to the prediction that the *TRF4*/Pol  $\sigma$  gene family is distantly related to the  $\beta$ -polymerase superfamily (ARAVIND and KOONIN 1999), which consists of proteins that catalyze a variety of nucleotidyltransferase reactions, including DNA synthesis. The homology was discovered using iterative database searches combined with computer modeling based on the crystal structure of known  $\beta$ -polymerase family members (ARAVIND and KOONIN 1999). Homology is not apparent in standard "BLAST" database searches. It is important to determine the significance of this predicted structural similarity since some small molecule inhibitors of Pol  $\beta$  have anti-

<sup>1</sup>Present address: The Johns Hopkins Oncology Center, Molecular Genetics Laboratory, Baltimore, MD 21231.

<sup>2</sup>Present address: Department of Molecular Biology and Genetics, Johns Hopkins University, Baltimore, MD 21205-2185.

<sup>3</sup>Corresponding author: Department of Genetics and Genomics, E603, Boston University Medical Center, 715 Albany St., Boston, MA 02118. E-mail: mfc@bu.edu

tumor activity (Hsu *et al.* 1997; DENG *et al.* 1999). In addition, a genetic analysis will allow us to better define those regions of *TRF4*/Pol  $\sigma$  required for its various roles in cohesion and DNA repair.

Here we present a thorough genetic analysis of *TRF4*/Pol  $\sigma$ . The data strongly support the prediction that regions of structural similarity to the  $\beta$ -polymerase superfamily are important for *TRF4*/Pol  $\sigma$  function. Furthermore, the analysis defines a C-terminal domain that is also essential for *TRF4*/Pol  $\sigma$  function.

## MATERIALS AND METHODS

**Site-directed mutagenesis:** The *TRF4* gene was cloned into a pALTER-derived phagemid vector (Promega, Madison, WI) containing the *HIS3* gene (CB905) and site-directed mutagenesis was carried out using the Altered Sites II *in vitro* mutagenesis system (Promega). The *trf4* alleles produced by this method were sequenced (Biomolecular Research Facility, University of Virginia) to confirm the presence of the desired mutation. Sequences of mutagenic oligos are available upon request.

**Integration of *trf4* mutant alleles by one-step gene replacement:** Fragments containing mutant *trf4* alleles and the *HIS3* marker were isolated by digesting the mutated plasmid with *Mlu*I and *Not*I restriction enzymes. The linear fragments were transformed into the recipient strain CY1035 (*MATa trf4 $\Delta$ ::TRP1 trf5 $\Delta$ ::LEU2 pTRF5.URA3*). Integrants that replace the parent *trf4 $\Delta$ ::TRP1* allele with the *trf4* surface-targeted allele linked to *HIS3* were selected on SC-his plates. Colonies were then purified on SC-his plates and tested for their growth on SC-trp medium to confirm that the parental *trf4::TRP1* allele had been replaced. Mutant alleles that are integrated correctly at the normal *TRF4* locus should be His<sup>+</sup> and Trp<sup>-</sup> since the *trf4* allele linked to *HIS3* should have replaced the *trf4::TRP1* allele on chromosome XV (Figure 1A). The genomic structure of the candidate mutant strains was further confirmed by PCR analysis (not shown).

**Western blotting:** Yeast were grown to log phase in YPD medium. Cell extracts were made by glass-bead disruption (DUNN and WOBBE 1997), run on an 8% SDS-PAGE gel, and transferred to a nitrocellulose membrane. The nitrocellulose membrane was blocked with 5% milk-Tris-borate SDS (TBS) and incubated for 1 hr with a rabbit anti-Trf4p polyclonal antibody, followed by a 1-hr incubation with secondary antibody. The membrane was washed three times with TBS before and after adding the second antibody. Immunoreactive bands were visualized by enhanced chemiluminescence (Amersham, Buckinghamshire, UK).

**Exonuclease activity assays:** *Cofractionation with polymerase:* DNA polymerase assays were performed with 1- $\mu$ l aliquots of each fraction. The oligo(dT) primer was end labeled using T4 polynucleotide kinase. Aliquots were incubated with 100 nm oligo(dT)/poly(dA) [20:1 molar excess of poly(dA): oligo(dT)] for 5 min at 37° in 50 mM Tris-HCl pH 8.0 (pH at 22°), 10 mM MgCl<sub>2</sub>, 2 mM dithiothreitol, 20 mM NaCl, 20 mM KCl, 2.5% glycerol, 0.2 mg/ml BSA, and 1 mM deoxy thymidine triphosphate (dTTP).

*Metal dependency:* A 35-mer primer was 5' labeled with <sup>32</sup>P and hybridized with a 75-mer template to form the exonuclease substrate as described in Z. WANG *et al.* (2000). Exonuclease reactions were performed for 30 min at 37° in 50 mM Tris-HCl pH 8.0 (pH at 22°), 10 mM MgCl<sub>2</sub>, 2 mM dithiothreitol, 20 mM NaCl, 20 mM KCl, 2.5% glycerol, 0.2 mg/ml BSA, and 1 mM dTTP. Reaction products were resolved on an 8 M urea/20% acrylamide gel.

**Chromosome spreads:** Chromosome spreads were performed as described (MICHAELIS *et al.* 1997) with the following minor modifications. Cells were grown in YPD to early log phase and 10 ml of the culture was harvested, washed in spheroplasting solution (1.2 M sorbitol, 0.1 M potassium phosphate pH 7.4, 0.5 M MgCl<sub>2</sub>), and then digested in the same solution containing 0.5% 2-mercaptoethanol and 50  $\mu$ g/ $\mu$ l zymolyase 100-T (ICN Biomedicals) at 23° for 10 min. The digestion was stopped and the cells were spread as described (MICHAELIS *et al.* 1997).

**Tubulin immunofluorescence:** Mitotic spindles were visualized by immunofluorescence as previously described (CASTAÑO *et al.* 1996), using an antibody to yeast  $\alpha$ -tubulin, YOL1/34 (Serotec, Oxford), and a Texas red-conjugated secondary antibody. Cells were viewed using a Nikon Eclipse 800 epifluorescence microscope. Images were captured digitally using a Princeton Instruments camera and IP Lab Spectrum software.

**GFP chromosome tagging assay for sister chromatid cohesion:** Sister chromatid cohesion was monitored essentially as described in STRAIGHT *et al.* (1996). Yeast strains containing the *lacO* repeat integrated at the *LEU2* locus, and the *GFP-lacI* fusion under the *HIS3* promoter integrated at the *HIS3* locus, were grown overnight in SC-histidine at 30°. Cells were diluted to an A<sub>600</sub> of 0.2 and allowed to double once more. Cells were spun and resuspended in the same volume of YPD plus 20  $\mu$ g/ml of nocodazole or 25  $\mu$ g/ml of  $\alpha$ -factor. After 4 hr, cells were fixed by adding 0.1 volume of 37% formaldehyde and incubated for 5 min. Cells were then collected by centrifugation in a microfuge and washed three times with water. The cell suspension was diluted and sonicated briefly, cells were then adhered to polylysine-coated slides, and 5  $\mu$ l of antifade solution with 4',6-diamidino-2-phenylindole (DAPI) was added to each well. Slides were viewed and images were captured as described above. A GFP LP filter from Chroma Technology (Brattleboro, VT) was used to visualize the GFP signal.

## RESULTS

**Systematic construction of “surface-targeted” mutations in *TRF4*:** On the basis of iterative database searching and structural modeling (ARAVIND and KOONIN 1999) it has been proposed that the Trf4p/Pol  $\sigma$  DNA polymerase family of proteins is distantly related to the  $\beta$ -polymerase superfamily of nucleotidyltransferases. However, virtually no primary amino acid sequence similarity is evident upon alignment of the two sequences despite the fact that both encode DNA polymerases. To determine the importance of these regions to *TRF4* function, we constructed 34 “surface-targeted” mutations in *TRF4* and examined their phenotypes.

Surface-targeted mutagenesis is based on the assumption that clusters of charged residues are likely to reside on a protein's surface and not in the hydrophobic interior (WERTMAN *et al.* 1992). “Surface regions” of a protein are predicted by screening the primary sequence of amino acids for the presence of two or more charged residues in a window of any five amino acids. Each of the charged residues in a predicted surface region is then changed to alanine by site-directed mutagenesis. Mutagenic oligos were synthesized and site-directed mutagenesis was performed to make the 34 mutant alleles of *TRF4* that alter predicted surface regions (Table 1

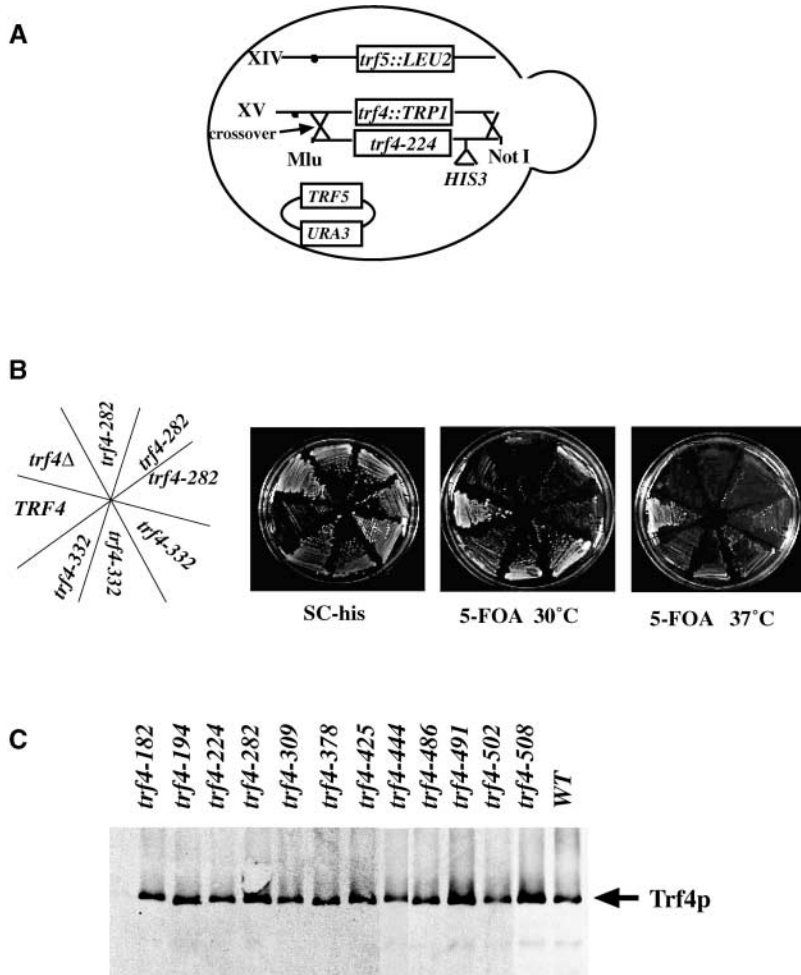


FIGURE 1.—Construction of Trf4/Pol  $\sigma$  “surface-targeted” mutants: (A) The scheme used to integrate each of the *trf4* surface-targeted mutant alleles into the natural *TRF4* chromosomal locus. This was performed by transformation of CY1187 with a linear DNA fragment (*MluI*-*NotI*) carrying the *trf4* mutant allele and the *HIS3* gene cloned 3' to the *TRF4* open reading frame (Table 1). His<sup>+</sup> transformants were isolated and screened to identify those that had simultaneously become Trp<sup>-</sup>. Correct genomic structure was confirmed by PCR analysis of genomic DNA from candidate transformants using primers that flank the *TRF4* locus. (B) CY1187 (*TRF4::HIS3*), CY1035 (*trf4Δ::TRP1*), CY1291 (*trf4-282::HIS3*), and CY1297 (*trf4-332::HIS3*) were streaked onto SC-his plates at 30° and 5-FOA plates at both 30° and 37° and incubated for 3 days. Only those cells that lost the *URA3* plasmid were able to grow on 5-FOA-containing medium (BOEKE *et al.* 1984). (C) Strains carrying the following mutant alleles of *TRF4*: *trf4-182* (CY1193), *trf4-194* (CY1194), *trf4-224* (CY1625), *trf4-282* (CY1291), *trf4-309* (CY1296), *trf4-378* (CY1264), *trf4-425* (CY1248), *trf4-444* (CY1295), *trf4-486* (CY1196), *trf4-491* (CY1270), *trf4-502* (CY1293), *trf4-508* (CY1294), and wild-type (CY184) strains were grown to log phase and cell extracts were made. Western blots were performed to detect Trf4p using a polyclonal antibody to the C-terminal 15 amino acids.

and Figure 2). Each allele was then integrated into the natural *TRF4* locus by single-step gene replacement made possible by the presence of a selectable *HIS3* gene inserted 84 nucleotides 3' to the *TRF4* stop codon (Figure 1A). Western blots confirmed that mutant strains produced normal levels of Trf4p (Figure 1C). Mutants carrying each of the 34 *trf4* mutant alleles were then examined in both *TRF5* and *trf5* mutant backgrounds for a variety of phenotypes including cell viability, double-strand break (DSB) repair capacity, sister chromatid cohesion, and chromosome association. The most amino-terminal amino acid mutated in a given charge cluster on Trf4p was used to designate the allele number.

**The  $\beta$ -polymerase-like domains in *TRF4* are essential for its function:** We have previously shown that a null mutation in *trf4* is lethal in combination with a *trf5* null mutation (CASTAÑO *et al.* 1996). The predicted Trf4p and Trf5p proteins are 55% identical and 72% similar and clearly act as redundant homologs. Thus, we examined the viability of the 34 surface-targeted mutant alleles of *TRF4* in a *trf5Δ* background to define those regions of *TRF4* needed for its essential function.

To facilitate construction of yeast strains carrying mu-

tant alleles of *trf4* at the normal *TRF4* locus in a *trf5Δ* background, we generated a *trf4Δ::TRP1 trf5Δ::LEU2* double-mutant strain covered with a *TRF5.URA3* plasmid to make the strain viable (CY1035, shown schematically in Figure 1A). Transformants that replace the parent *trf4-TRP1* allele with the *trf4* surface-targeted allele linked to *HIS3* were selected as described in MATERIALS AND METHODS.

The viability of mutants carrying a *trf4* allele was then examined by streaking three independent colonies of each mutant on SC plates containing (5-fluoroorotic acid 5-FOA) to select cells that have spontaneously lost the p*TRF5.URA3* cover plasmid (BOEKE *et al.* 1984). Thus, the inability of an integrant to give rise to 5-FOA-resistant segregants indicates that the mutant allele confers a lethal phenotype.

Examples of the analysis of 2 of the 34 alleles are shown in Figure 1B. A positive control with a wild-type *TRF4* locus readily yields 5-FOA-resistant segregants and a negative control carrying a *trf4* null mutation fails to yield 5-FOA-resistant segregants as expected (Figure 1B). The three independent *trf4-282* transformants are His<sup>+</sup>, but are unable to give rise to 5-FOA-resistant seg-

TABLE 1  
Surface-targeted *trf4* mutant yeast strains

| Strain | Allele          | Amino acid changes         | Plasmid | CPT <sup>a</sup> sensitivity | Viability in $\Delta trf5$ background |
|--------|-----------------|----------------------------|---------|------------------------------|---------------------------------------|
| CY1187 | <i>TRF4</i>     | None                       | CB905   | No                           | Viable                                |
| CY1181 | <i>trf4-12</i>  | K12A, K13A, K15A           | CB1084  | No                           | Viable                                |
| CY1182 | <i>trf4-21</i>  | K21A, K23A, K24A           | CB1085  | No                           | Viable                                |
| CY1183 | <i>trf4-78</i>  | D78A, D79A, D80A           | CB1086  | No                           | Viable                                |
| CY1186 | <i>trf4-101</i> | E101A, E102A, E104A        | CB1088  | No                           | Viable                                |
| CY1184 | <i>trf4-121</i> | D121A, D122A               | CB1087  | No                           | Viable                                |
| CY1197 | <i>trf4-131</i> | E131A, D132A, E133A        | CB1081  | No                           | Slow growth                           |
| CY1249 | <i>trf4-140</i> | E140A, R141A, E142A        | CB1100  | No                           | Slow growth                           |
| CY1261 | <i>trf4-145</i> | E145A, E147A               | CB1128  | No                           | Viable                                |
| CY1193 | <i>trf4-182</i> | E182A, K184A, D185A        | CB1089  | Yes                          | Lethal                                |
| CY1194 | <i>trf4-194</i> | E196A, E198A, R194A, E195A | CB1090  | Yes                          | Lethal                                |
| CY1251 | <i>trf4-217</i> | D217A, D219A               | CB1093  | No                           | Slow growth                           |
| CY1625 | <i>trf4-224</i> | G224A, S225A               | CB1354  | Yes                          | Lethal                                |
| CY1262 | <i>trf4-236</i> | D236A, D238A               | CB1129  | Yes                          | Lethal                                |
| CY1252 | <i>trf4-248</i> | K248A, E249A, R251A        | CB1091  | No                           | Viable                                |
| CY1263 | <i>trf4-262</i> | K262A, K263A, K264A        | CB1130  | No                           | Viable                                |
| CY1295 | <i>trf4-275</i> | K275A, R277A               | CB1135  | No                           | Temperature sensitive                 |
| CY1291 | <i>trf4-282</i> | K282A, E285A               | CB1134  | Yes                          | Lethal                                |
| CY1296 | <i>trf4-309</i> | R309A, E310A               | CB1137  | No                           | Lethal                                |
| CY1292 | <i>trf4-332</i> | R332A, R333A               | CB1132  | No                           | Temperature sensitive                 |
| CY1200 | <i>trf4-369</i> | K369A, D370A               | CB1099  | No                           | Viable                                |
| CY1264 | <i>trf4-378</i> | E378A, E381A               | CB1126  | Yes                          | Lethal                                |
| CY1269 | <i>trf4-390</i> | D390A, D391A               | CB1096  | No                           | Viable                                |
| CY1248 | <i>trf4-425</i> | D425A, D428A, E429A        | CB1121  | No                           | Lethal                                |
| CY1195 | <i>trf4-444</i> | K444A, K445A               | CB1094  | Yes                          | Lethal                                |
| CY1265 | <i>trf4-467</i> | K467A, D468A, R469A        | CB1131  | No                           | Temperature sensitive                 |
| CY1196 | <i>trf4-486</i> | R486A, D487A, D490A        | CB1095  | No                           | Lethal                                |
| CY1270 | <i>trf4-491</i> | E491A, R492A               | CB1097  | Yes                          | Lethal                                |
| CY1293 | <i>trf4-502</i> | E502A, E504A               | CB1133  | No                           | Lethal                                |
| CY1294 | <i>trf4-508</i> | K508A, K509A, R510A        | CB1136  | Yes                          | Lethal                                |
| CY1259 | <i>trf4-521</i> | E521A, D522A               | CB1124  | No                           | Viable                                |
| CY1267 | <i>trf4-545</i> | K545A, K546A, K548A        | CB1122  | No                           | Viable                                |
| CY1266 | <i>trf4-554</i> | K554A, E556A               | CB1127  | No                           | Viable                                |
| CY1268 | <i>trf4-559</i> | K559A, R560A               | CB1123  | No                           | Slow growth                           |
| CY1199 | <i>trf4-572</i> | E572A, D573A, D574A        | CB1098  | No                           | Slow growth                           |

All strains are isogenic with CY1187 (*MATa TRF4-HIS3 trf5::LEU2 his3-11,15 leu2-3,112 trp1-1 ura3-1 ade2-1 + pURA3.TRF5*) with the exception of the *trf4* allele. Plasmids used for integration of the *trf4* mutants are listed.

<sup>a</sup> Camptothecin sensitivity in a *TRF5* background. Strains that are CPT sensitive are at least 10-fold more sensitive to the drug than the wild-type strain.

regants at either 30° or 37°. This indicates that the *trf4-282* mutation abolishes the essential function of *TRF4* at both 30° and 37°. In contrast, the *trf4-332* mutant does yield slow-growing 5-FOA-resistant segregants at 30°, indicating that it causes a growth defect but does not eliminate the essential function. However, at 37° the *trf4-332* mutant does not yield 5-FOA-resistant segregants. Thus, *trf4-332* confers a growth defect at 30° and a temperature-sensitive inviability at 37°. A similar analysis was performed for all 34 mutant alleles in *TRF4*.

Of the 34 alleles that were integrated at the *TRF4* locus in a *trf5* mutant background, 13 are inviable, 8 display temperature-sensitive growth or a growth defect as observed by significantly slower colony formation compared to the wild-type parent, and 13 have no obvi-

ous growth defect. Western blot analysis of the 13 inviable mutants demonstrates that each produces wild-type levels of Trf4p (Figure 1C). Thus, the mutants are defective for *TRF4* function and not simply for protein stability.

The eight regions of predicted structural similarity between the  $\beta$ -polymerase superfamily and *TRF4* (ARAVIND and KOONIN 1999) are underlined and numbered in Figure 2 to show the positions of these regions with respect to the surface-targeted mutations in *TRF4*. Ten mutations lie in the eight  $\beta$ -polymerase-like regions. Of these, 7 are inviable and 3 show growth defects. In contrast, of the 5 mutations that lie between, but not within, the eight  $\beta$ -polymerase-like regions, 4 have no obvious phenotype and 1 is inviable. This striking contrast clearly

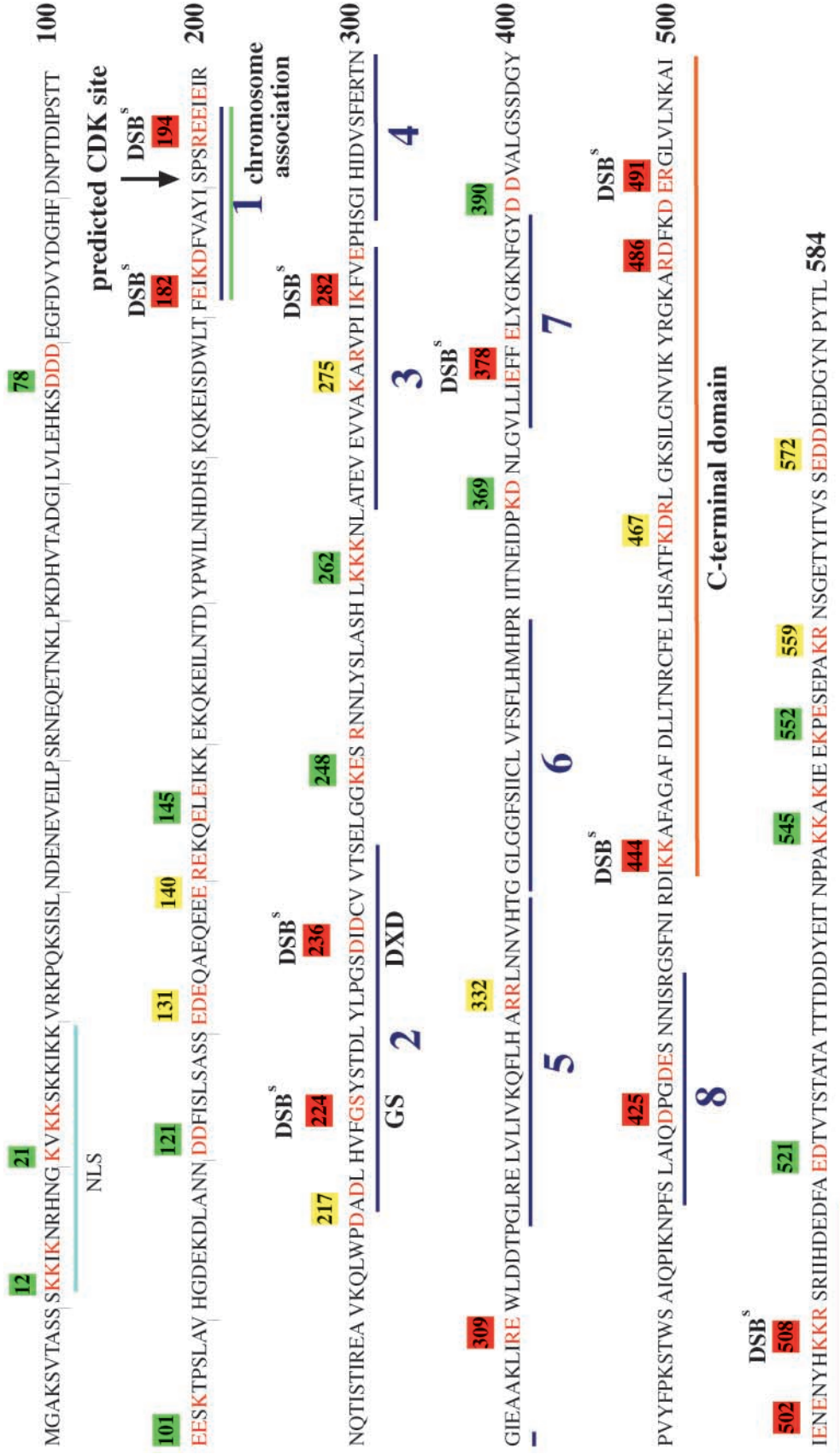


FIGURE 2.—Phenotypes and locations of surface-targeted mutant alleles in *TRF4*. The position of each of the 34 surface-targeted mutations in *TRF4* is marked with the allele number. Each allele number corresponds to the most amino-terminal residue that is mutated to alanine. The specific residues changed to alanine are shown in red in the primary sequence. The allele numbers are highlighted in green for those that do not affect viability in a *trf5* background, yellow for those that cause a growth defect or temperature sensitivity, and red for those that are inviable in the absence of *TRF5*. Mutations that cause CPT hypersensitivity in a *TRF5* background are designated as DSB<sup>s</sup>. The eight regions of predicted structural similarity between Trf4p/Pol σ and the Pol β superfamily are underlined in blue and marked with Arabic numerals. The five lethal mutations clustered outside the polymerase domains are underlined and labeled “C-terminal domain.”

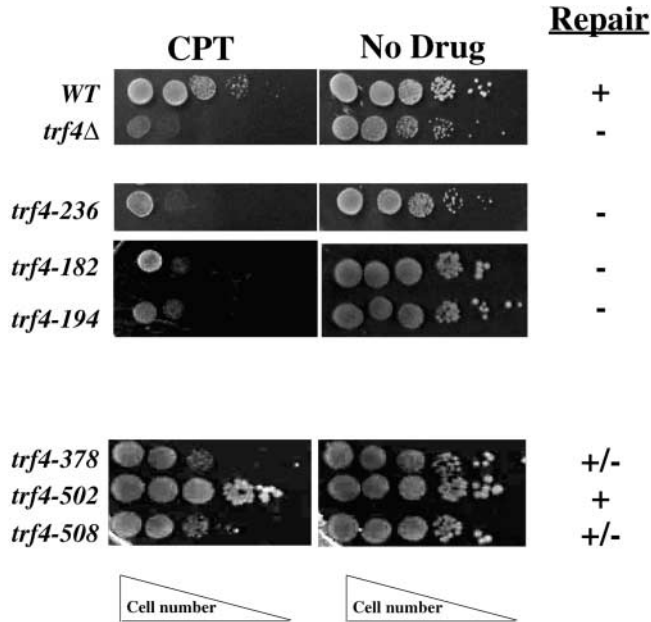


FIGURE 3.—Regions of Trf4p/Pol  $\sigma$  are required for repair. *trf4Δ* (CY1000), *trf4-236* (CY1262), *trf4-182* (CY1193), *trf4-194* (CY1194), *trf4-378* (CY1264), *trf4-502* (CY1293), *trf4-508* (CY1294), and wild-type (CY184) strains were grown to mid-log phase in YPD and serial 10-fold dilutions were spotted onto plates containing 10  $\mu$ g/ml camptothecin or with no drug. Plates were incubated at 30° for 3 days.

shows the importance of the predicted Pol  $\beta$ -like domains for the essential function of *TRF4*/Pol  $\sigma$ .

The C terminus and central polymerase domain are highly evolutionarily conserved, whereas the N terminus is not. Of the eight mutations constructed in the N-terminal region, all remain viable in the absence of *TRF5*: Six have no obvious phenotype and two show a growth defect. In contrast, the conserved C-terminal region (amino acids 436–584), which lies outside the polymerase domain, is critical for the common essential function between *TRF4* and *TRF5*, because five of the inviable mutant alleles occur in this region.

**The DNA polymerase and C-terminal domains are required for *TRF4*'s role in DNA damage repair:** A null mutant strain of *trf4* is hypersensitive to the DNA-damaging agents camptothecin (CPT) and methyl methanesulfonate (MMS) even in the presence of *TRF5* (WALOWSKY *et al.* 1999; Figure 3). Both CPT and MMS induce S-phase-specific DNA lesions that cause subsequent collapse of approaching replication forks (HSAING *et al.* 1989; LIU 1989; SCHWARTZ 1989; NITISS and WANG 1996; TERCERO and DIFFLEY 2001). Since DSB repair pathways are required for resistance to MMS and the repair of replication-fork-associated DSB caused by CPT (XIAO *et al.* 1996; ARNAUDEAU *et al.* 2001), it is likely that *TRF4* is necessary for DSB repair. To determine whether the surface-targeted mutations are defective for this repair, all of the *trf4* mutant alleles were integrated into the natural *TRF4* locus in a *TRF5* background, and mutant

strains were assayed for their sensitivity to CPT (Figure 3). Mutant strains were grown to log phase and serial 10-fold dilutions were made on plates containing CPT.

The mutants show a spectrum of repair capacity. For example, the *trf4-182* mutant is defective for DNA repair, whereas the *trf4-502* allele is not. Analysis of all 34 mutants indicates that the regions of Trf4p/Pol  $\sigma$  required for CPT resistance are a subset of the essential regions of the gene. Of the 13 alleles that are inviable in combination with *trf5*, 9 of these are repair defective in a *TRF5* background (at least 10-fold more sensitive to CPT than the wild-type parent strain). In contrast, none of the 21 viable mutants have a repair defect. Alleles that are repair defective are marked “DSB” in Figure 2. These mutations reside in both the DNA polymerase and C-terminal domains, but not in the N-terminal domain.

Crystal structures of  $\beta$ -polymerase superfamily proteins indicate that the conserved “GS...DXD” motif forms a metal-binding site that is crucial for their polymerase activity (PELLETIER *et al.* 1994; SAWAYA *et al.* 1994). We mutated the DXD motif (*trf4-236*) and found that it greatly diminishes the DNA polymerase activity *in vitro* (Z. WANG *et al.* 2000). The data in Figure 3 show that the *trf4-236* mutant is camptothecin sensitive, demonstrating that polymerase activity is required for Trf4p/Pol  $\sigma$ 's repair function. Consistent with this, another polymerase motif mutant, *trf4-224*, which mutates the GS residues to alanine, is also repair defective (data not shown). In addition, another four mutants within the polymerase domain are repair defective, suggesting that the DNA polymerase domain plays a crucial role in *TRF4*'s DNA repair function.

However, the DNA polymerase domain alone is not sufficient for DNA repair, because the *trf4-444*, *trf4-491*, and *trf4-508* mutants, which alter amino acids outside the polymerase domain, are also repair defective. Each of these alleles resides in the C-terminal domain, further demonstrating the importance of this region in *TRF4* function.

**Trf4p/Pol  $\sigma$  displays 3' to 5' exonuclease activity *in vitro*:** During purification of recombinant Trf4p from *Escherichia coli* we observed consistent cofractionation of an exonuclease activity through the final purification step. In Figure 4A, lanes 6 and 7, cofractionation of Trf4p with DNA polymerase activity and a truncated 5'-end-labeled primer (arrow at bottom of Figure 4A) are observed. To investigate this further, assays of purified recombinant protein were performed using a substrate consisting of a 75-mer annealed to a complementary, 5'-end-labeled 35-mer primer. These assays show that incubation of purified Trf4p with the oligo/labeled primer in the absence of dNTPs results in removal of nucleotides from the 3' end of the primer (Figure 4B). Thus, Trf4p possesses 3' to 5' exonuclease activity. The activity does not require ATP (lane 4), but is completely dependent on exogenous  $Mg^{2+}$  (lanes 4 and 7). Neither  $Mn^{2+}$  (lane

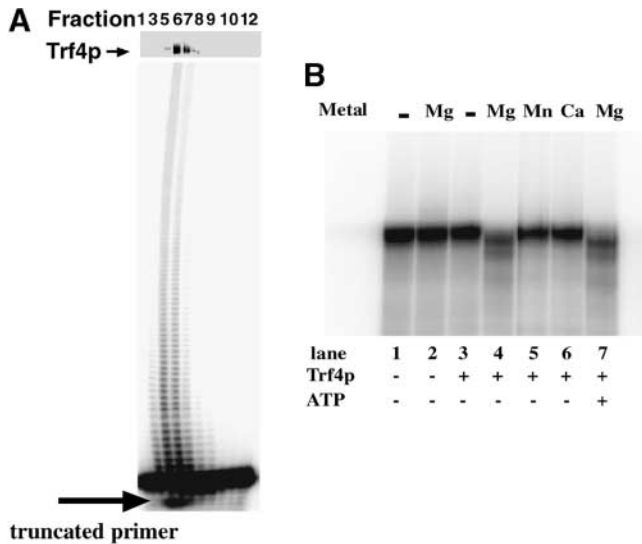


FIGURE 4.—Trf4/Pol  $\sigma$  displays  $Mg^{2+}$ -dependent exonuclease activity *in vitro*. (A, top) A Coomassie-stained SDS-PAGE gel of the Trf4p fractions eluted from a Mono Q column following ammonium sulfate and Ni-agarose affinity chromatography (Z. WANG *et al.* 2000). The oligo(dT) primer is the dark band near the bottom of the gel while a truncated primer (arrow), the product of the exonuclease activity, is observed just below full-length oligo(dT) primer. (B) A 35-mer primer was 5' labeled with  $^{32}P$  and hybridized with a 75-mer template as in Z. WANG *et al.* (2000). Trf4p was added to lanes 3–7;  $Mg^{2+}$  was added to lanes 2, 4, and 7;  $Mn^{2+}$  was added to lane 5; and  $Ca^{2+}$  was added to lane 6; and 1 mM ATP was added to lane 7. Reaction products were resolved on an 8 M urea/20% acrylamide gel and autoradiography was performed.

5) nor  $Ca^{2+}$  (lane 6) are effective substitutes for  $Mg^{2+}$  in the assay.

**Cell-cycle-regulated association of Trf4p/Pol  $\sigma$  with chromosomes:** To begin to understand whether Trf4p/Pol  $\sigma$  associates with other chromosome-bound proteins, we sought to identify the regions of Trf4p/Pol  $\sigma$  required for its chromosome localization. Association of nuclear proteins with chromosomes can be monitored using the chromosome spread method (MICHAELIS *et al.* 1997). Cells are partially fixed, lysed, and then extensively washed such that all cytoplasm and nucleoplasm are removed. Under these conditions only chromatin-associated proteins remain and their presence can be detected by immunostaining.

To monitor Trf4p/Pol  $\sigma$  chromosome association, we used a strain that expresses Trf4p epitope tagged with two repeats of the IgG-binding domain of protein A, referred to as “TRF4-ZZ” (CY1344), and visualized the protein using FITC-coupled IgG. The association of the wild-type protein with chromosomes is readily detected as expected (Figure 5A). Negative controls included a strain with an untagged *TRF4* gene that carried the ZZ vector (CY1346) and a strain carrying cytoplasmically located Pho4-ZZ mutant protein (CY1349). Chromosome spreads were then performed on the nuclei from

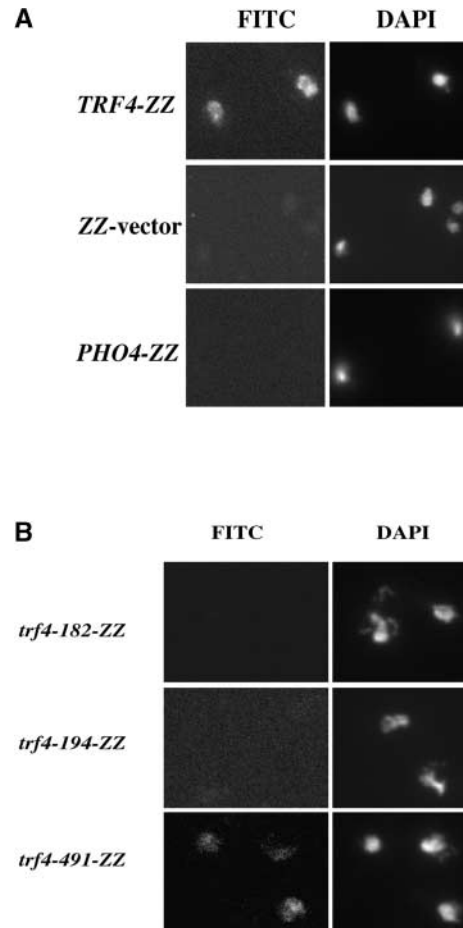


FIGURE 5.—Trf4p/Pol  $\sigma$  binds to chromosomes. (A) *TRF4-ZZ* (CY1344), *ZZ-vector* (CY1346), and *PHO4-ZZ* strains (CY1349) were grown to log phase and then fixed to perform chromosome spreads. The ZZ-tagged protein was visualized with FITC-conjugated rabbit IgG. DNA was visualized with DAPI. (B) A small region of Trf4p is required for chromosomal association. The chromosome spread assay was performed as in A. The *trf4-182-ZZ* (CY1435) and *trf4-194-ZZ* (CY1436) mutants fail to associate with chromosome spreads, whereas the *trf4-491-ZZ* mutant (CY1432) remains associated.

the 13 *trf4* charge-to-alanine mutants that we knew to be lethal in combination with a *TRF5* deletion. To do this, each allele was fused in frame to the ZZ epitope tag either at the natural *TRF4* locus or at the *TRP1* locus in a *trf4* deletion background, so that chromosome association could be monitored (MATERIALS AND METHODS and Table 2).

Of the 13 mutant Trf4 proteins examined, 11 retain their ability to bind to chromosomes. However, the *trf4-182-ZZ* and *trf4-194-ZZ* alleles produced proteins that completely failed to associate with chromosomes in chromosome spreads (Figure 5B) despite the fact that the proteins are made at normal levels (Figure 1C). Thus, a relatively discrete region of *TRF4* is critical for its binding to chromosomes. Intriguingly, this region flanks the only cyclin-dependent kinase consensus phosphorylation site in the protein at serine 191, suggesting

**TABLE 2**  
**Other yeast strains used in this study**

| Strain | Relevant genotype                                                                       |
|--------|-----------------------------------------------------------------------------------------|
| CY184  | Wild type                                                                               |
| CY1000 | <i>trf4::HIS3</i>                                                                       |
| CY1244 | <i>his3::GFP-LacI::HIS3 leu2:(LacO)<sub>256</sub>::LEU2</i>                             |
| CY1247 | <i>trf4::TRP1 his3::GFP-LacI::HIS3 leu2:(LacO)<sub>256</sub>::LEU2</i>                  |
| CY1344 | <i>trp1::TRF4-ZZ-TRP1 trf4::HIS3</i>                                                    |
| CY1346 | <i>trp1::ZZ vector-TRP1 trf4::HIS3</i>                                                  |
| CY1349 | <i>trp1::PHO4-ZZ-TRP1 trf4::HIS3</i>                                                    |
| CY1350 | <i>trp1::trf4-486-ZZ-TRP1 trf4::HIS3</i>                                                |
| CY1351 | <i>trf4-182-HIS3 his3::GFP-LacI::HIS3 leu2:(LacO)<sub>256</sub>::LEU2</i>               |
| CY1355 | <i>trf4-491-HIS3 his3::GFP-LacI::HIS3 leu2:(LacO)<sub>256</sub>::LEU2</i>               |
| CY1432 | <i>trp1::trf4-491-ZZ::TRP1 trf4::HIS3</i>                                               |
| CY1433 | <i>trp1::trf4-502-ZZ-TRP1 trf4::HIS3</i>                                                |
| CY1434 | <i>trp1::trf4-508-ZZ-TRP1 trf4::HIS3</i>                                                |
| CY1435 | <i>trf4-182-ZZ-TRP1::HIS3</i>                                                           |
| CY1436 | <i>trf4-194-ZZ-TRP1::HIS3</i>                                                           |
| CY1437 | <i>trf4-236-TRP1::HIS3</i>                                                              |
| CY1438 | <i>trf4-282-ZZ-TRP1::HIS3</i>                                                           |
| CY1439 | <i>trf4-309-ZZ-TRP1::HIS3</i>                                                           |
| CY1440 | <i>trf4-378-ZZ-TRP1::HIS3</i>                                                           |
| CY1441 | <i>trf4-425-ZZ-TRP1::HIS3</i>                                                           |
| CY1442 | <i>trf4-444-ZZ-TRP1::HIS3</i>                                                           |
| CY1447 | <i>trp1::TRF4-ZZ-TRP1 trf4::HIS3 cdc15-2</i>                                            |
| CY1451 | <i>trf4-194-ZZ-TRP1 trf4::HIS3 his3::GFP-LacI::HIS3 leu2:(LacO)<sub>256</sub>::LEU2</i> |
| CY1658 | <i>trf4-224-ZZ-TRP1::HIS3</i>                                                           |

that phosphorylation of Trf4p may be important for its chromosome association. Indeed, an activating mutation in the yeast cyclin-dependent kinase *CDC28-Y19F* suppresses the temperature-sensitive growth defect of a *trf4-ts trf5* strain (I. B. CASTAÑO, C. ADAMS and M. F. CHRISTMAN, unpublished observation), but the mechanism of suppression remains to be determined.

To determine whether Trf4p is chromosome associated at all points in the cell cycle, we monitored the association of Trf4p with chromosome spreads throughout the course of a single synchronous cell cycle. G1 daughter cells obtained by centrifugal elutriation were released into fresh medium and monitored every 30 min thereafter for the presence of Trf4p on chromosome spreads, for nuclear morphology, and for spindle morphology (Figure 6A). Association of Trf4p with chromosomes begins ~30 min after release, becomes stronger at 60 min (onset of DNA synthesis; not shown), and continues through 90 min. At 120 min after release the metaphase-to-anaphase transition takes place as evidenced by the presence of highly elongated anaphase spindles. Coincident with the metaphase-to-anaphase transition, Trf4p's association with chromosome spreads is abolished.

To further examine the apparent dissociation of Trf4p from chromosomes at the metaphase-to-anaphase transition we compared metaphase- and telophase-arrested cells for Trf4-ZZp association with chromosomes. A strain containing Trf4-ZZp and a temperature-sensitive *cdc15-2* mutation (CY1447) was grown at permissive tempera-

ture and treated with nocodazole to synchronize cells in metaphase. To achieve telophase arrest, cells were shifted to the nonpermissive temperature (37°) for 3 hr (KABACK *et al.* 1984). As shown in Figure 6B, Trf4-ZZp is associated with metaphase chromosome preparations but is nearly absent from telophase chromosome preparations. Quantitation of 167 preparations from nocodazole-treated cells and 341 preparations from telophase-arrested cells shows that 95% of metaphase chromosome spreads stain intensely with FITC-conjugated IgG whereas only 10% of telophase spreads show any staining and the staining that is observed is generally weak. Wild-type *CDC15* controls demonstrate that Trf4-ZZp association is not lost simply due to the temperature shift to 37° (data not shown).

Western blot analysis of metaphase and telophase cell extracts shows that the level of the Trf4-ZZp protein is the same at both points in mitosis (Figure 6B). Thus, Trf4p is being removed from chromosomes in some manner and not simply degraded. The slight reduction of Trf4p in G1 cells must occur after its removal from chromosomes. This behavior is similar to the cohesin Scc1p/Mcd1p, which dissociates from chromosomes at the metaphase-to-anaphase transition prior to being degraded rapidly (MICHAELIS *et al.* 1997).

**Defective sister chromatid cohesion in *TRF4* point mutants:** If the Trf4-182 and Trf4-194 proteins have completely lost their ability to bind to chromosomes, then we anticipate that they would behave as null mu-

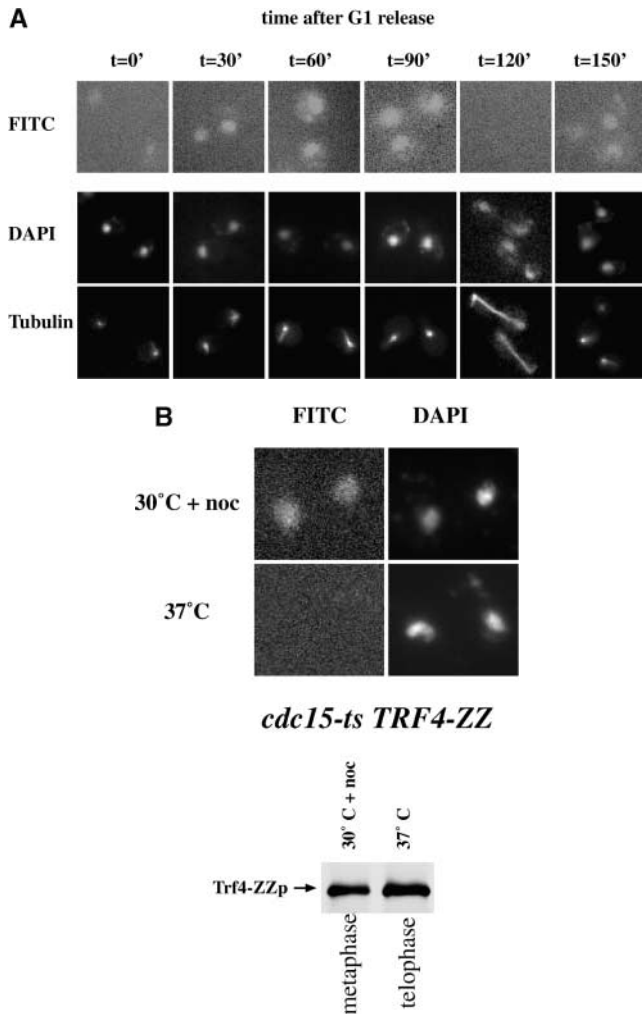


FIGURE 6.—Association of Trf4p/Pol  $\sigma$  with chromosomes is cell cycle regulated. (A) G1 cells of strain CY1344 expressing *TRF4-ZZ* were collected by elutriation and released into YPD at 30°. At the indicated times, samples were collected and fixed for chromosome spreads and tubulin immunofluorescence. (B, top) A strain containing *TRF4-ZZ* and a temperature-sensitive *cdc15-2* mutation (CY1447) was grown to log phase at 30° in YPD and either treated with 20  $\mu$ g/ml nocodazole for 3 hr or shifted to 37° for 3 hr. Cells were fixed for chromosome spreads and Trf4-ZZ protein was detected with FITC-conjugated rabbit IgG. DNA was visualized with DAPI. (Bottom) Cells were harvested after 3 hr in nocodazole or at 37°. Protein extracts were prepared and separated by SDS-PAGE and Trf4-ZZ proteins were detected by Western blot using anti-IgG antibodies.

tants. To address this we examined sister chromatid cohesion in the *trf4-182* and *trf4-194* mutants using the “GFP chromosome tagging assay” developed by Murray and colleagues (STRAIGHT *et al.* 1996). In the GFP chromosome assay, 256 tandem repeats of the *lac* operator are integrated on one of the yeast chromosomes and chromosomes are visualized using immunofluorescence microscopy to detect the GFP fluorescence signal generated from binding of a GFP-*lac* repressor fusion. Using this assay the status of sister cohesion can be monitored

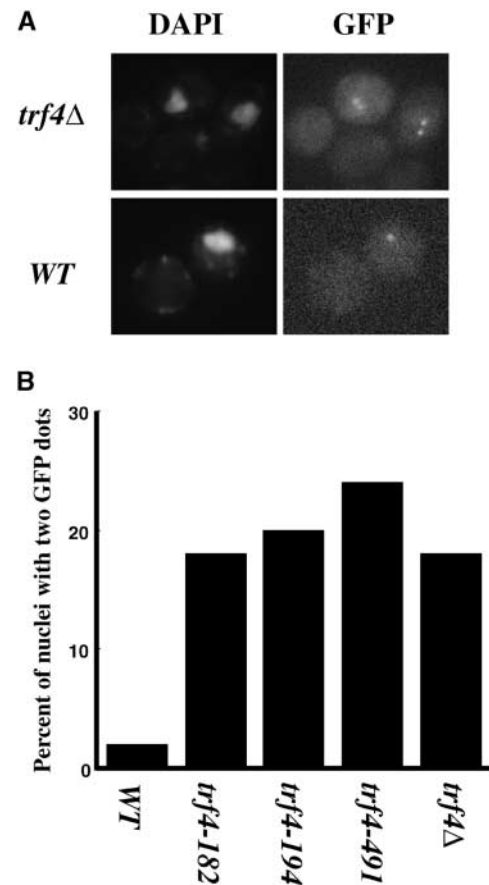


FIGURE 7.—Cohesion-defective alleles of Trf4/Pol  $\sigma$  reside in the polymerase and C-terminal domains. (A) Wild-type (CY1244) and *trf4 $\Delta$ ::TRP1* (CY1247) strains expressing a GFP-*lacI* fusion and containing 256 tandem repeats of *lacO* at the *LEU2* locus on chromosome III were grown in SC complete to early log phase. After induction of the GFP-*lacI* fusion, cells were pelleted, washed, and resuspended in YPD containing 20  $\mu$ g/ml nocodazole for an additional 4 hr. After the arrest, cells were fixed and adhered to glass slides. Cells were analyzed for the presence of one or two fluorescence signals. (B) Wild type (CY1244); *trf4 $\Delta$ ::TRP1* (CY1247); and strains containing alleles *trf4-182* (CY1351), *trf4-194* (CY1451), and *trf4-491* (CY1355) were analyzed as in A. Quantitation of the cohesion defects in each strain is shown.

by determining whether one or two fluorescence signals are observed within a single nucleus following DNA replication (STRAIGHT *et al.* 1996). We made the mutant strains with the *lac* operators integrated on chromosome III and *GFP-LacI* fusion integrated at the *HIS3* locus by a cross with a wild-type strain carrying those genes (Table 2). The wild-type strain showed a single GFP signal in nearly all of the cells examined. Of 110 nuclei examined, two signals were present in <2.5% of wild-type nuclei. In contrast, the *trf4* mutant cells showed a single signal in 82% of nuclei and two signals in 18% of nuclei (Figure 7, A and B). G1 controls were performed in all *trf4* mutants and confirm that the presence of two signals is not due to aneuploidy (data not shown). *trf4-182* and *trf4-194* mutants show two signals in 18 and 20% of

nuclei, respectively (Figure 7B). The cohesion defect in *trf4-182* and *trf4-194* is nearly identical to that of a *trf4* deletion, consistent with a failure of these alleles to bind chromosomes. Both alleles are CPT sensitive and cause inviability in a *trf5Δ* background. Thus, mutation near the cyclin-dependent kinase (CDK) consensus site results in null phenotypes, indicating that chromosome association is likely to be completely abolished.

While association of Trf4p with chromosomes is necessary for cohesion, it is clearly not sufficient. This conclusion stems from the observation that the *trf4-491-ZZ* mutant product associates normally with chromosome spreads (Figure 5B), but is nonetheless defective in cohesion (24% of cells at the nocodazole block, Figure 7B). Thus, Trf4p must associate with chromosomes but association alone is not sufficient for proper cohesion.

## DISCUSSION

While Pol  $\sigma$  and Pol  $\beta$  are likely to possess some level of structural similarity, the Pol  $\sigma$  family is clearly a distinct family of enzymes. *TRF4*/Pol  $\sigma$  genes are highly conserved in all eukaryotes and show much greater similarity to each other than any of the genes do to Pol  $\beta$ . For example, while the yeast and human Trf4p/Pol  $\sigma$  proteins are 39% identical and 51% similar in primary amino acid sequence (WALOWSKY *et al.* 1999), neither protein has significant primary amino acid similarity to its species' Pol  $\beta$ .

Genetic analysis of 34 surface-targeted mutations in *TRF4*/Pol  $\sigma$  has led to the following conclusions:

1. The regions of predicted structural similarity between Pol  $\sigma$  and Pol  $\beta$  are indeed critical to the function of *TRF4*/Pol  $\sigma$ . This finding validates the predicted structural similarity (ARAVIND and KOONIN 1999) in spite of the paucity of primary sequence homology between these two enzymes.
2. The analysis has identified a novel C-terminal domain in *TRF4*/Pol  $\sigma$  that lies primarily outside the polymerase homology. Five mutant alleles in this region demonstrate that it, too, is essential to the function of *TRF4*/Pol  $\sigma$ .
3. Both the polymerase and C-terminal domains are necessary for DSB repair.
4. A discrete area in the N-terminal region of Trf4p is critical for chromosome association.

**Functional significance of Trf4/Pol  $\sigma$  exonuclease activity:** Our genetic analysis of Trf4/Pol  $\sigma$  has uncovered a cluster of mutations outside of the polymerase domain that cause inviability in the absence of *TRF5* and additional defects in DNA repair and sister chromatid cohesion. Recent analysis of the recBCD enzyme has identified residues in the primary sequence that are crucial for exonuclease activity (J. WANG *et al.* 2000). A closer examination of the C-terminal region of Trf4/Pol  $\sigma$  revealed limited similarity with the recBCD exo-

nuclease domain (not shown), suggesting that the exonuclease activity we observed with Trf4/Pol  $\sigma$  *in vitro* has functional significance.

**Trf4/Pol  $\sigma$  activities required for DNA damage repair:** DSB repair is known to require the activity of both leading- and lagging-strand DNA polymerases (HOLMES and HABER 1999). We have previously shown that *TRF4* is also required for the repair of CPT- and MMS-induced lesions (WALOWSKY *et al.* 1999). The genetic data presented here demonstrate that the polymerase active site motifs, *trf4-236* (DXD) and *trf4-224* (GS), and several residues in the C terminus that may affect exonuclease activity, *trf4-444*, *trf4-491*, and *trf4-508*, are required for this repair.

It is possible that the repair defect is an indirect result of defective sister chromatid cohesion. However, the two mutant alleles located in the polymerase active site motif both cause hypersensitivity to CPT, consistent with a role for nucleotide polymerization *per se* in the repair process. All of the CPT-sensitive alleles are found within either a region of similarity with Pol  $\beta$ , including the polymerase active site motif, or the putative C-terminal exonuclease domain, suggesting that polymerase and exonuclease activities are both necessary for Trf4/Pol  $\sigma$ 's role in DNA repair. None of the mutant alleles located outside of these regions are CPT sensitive. Analysis of sister chromatid cohesion in the remaining CPT-sensitive mutants will resolve whether or not the repair defect is secondary to the cohesion defect.

**Cell-cycle-regulated association of Trf4/Pol  $\sigma$  with chromosomes:** Trf4/Pol  $\sigma$  is found associated with chromosomes from late G1 until late G2. The disappearance of Trf4/Pol  $\sigma$  from chromosomes coincides with spindle elongation at the metaphase-to-anaphase transition of mitosis. This is identical to what is observed with Scc1p/Mcd1p (MICHAELIS *et al.* 1997). The dissolution of cohesion allows sister chromatids to be separated by the pulling forces of the mitotic spindle. If the activities that maintain cohesion are not regulated, breakage of the chromosomes would result from pulling apart sister chromatids that are still "glued" together. The timed dissociation of Trf4/Pol  $\sigma$  from chromosomes suggests that its function also must be regulated for proper execution of these events in mitosis.

Only 2 of the 13 mutant alleles in *TRF4* that are inviable in a *trf5Δ* background abolish its association with chromosomes. These two alleles, *trf4-182* and *trf4-194*, flank a consensus CDK phosphorylation site in Trf4p at serine 191. This also defines "region 1" of the putative structural homology with Pol (Figure 2). The coincident positions of the CDK consensus site with the residues important for chromosome association indicate that Trf4p/Pol  $\beta$  function may be regulated in some way by CDK phosphorylation.

Establishment of cohesion between sister chromatids is coupled with replication fork passage. Emerging evidence suggests that this coupling represents more than

a coincident timing of independent events, but rather that the establishment of cohesion involves the active participation of replication-related activities (reviewed in CARSON and CHRISTMAN 2001). These include the Trf4p/Pol  $\sigma$  DNA polymerase; PCNA, a processivity clamp for some DNA polymerases; and a modified RFC clamp-loader complex. The genetic analysis of *TRF4*/Pol  $\sigma$  presented here provides us with tools for experiments aimed at determining how this is accomplished.

The authors thank Nikki Levin, David Pellman, Mitch Smith, and members of the Christman lab for helpful comments. We also thank Erin O'Shea, Bruce Futcher, and Gavin Sherlock for strains and plasmids. This work was supported by grants from the National Institutes of Health and the Human Frontiers Science Program to M.F.C.

#### LITERATURE CITED

- ARAVIND, L., and E. V. KOONIN, 1999 DNA polymerase beta-like nucleotidyltransferase superfamily: identification of three new families, classification and evolutionary history. *Nucleic Acids Res.* **27**: 1609–1618.
- ARNAUDEAU, C., C. LUNDIN and T. HELLEDAY, 2001 DNA double-strand breaks associated with replication forks are predominantly repaired by homologous recombination involving an exchange mechanism in mammalian cells. *J. Mol. Biol.* **307**: 1235–1245.
- BOEKE, J. D., F. LACROUTE and G. R. FINK, 1984 A positive selection for mutants lacking orotidine-5'-phosphate decarboxylase activity in yeast: 5-fluoro-orotic acid resistance. *Mol. Gen. Genet.* **197**: 345–346.
- CARSON, D. R., and M. F. CHRISTMAN, 2001 Evidence that replication fork components catalyze establishment of cohesion between sister chromatids. *Proc. Natl. Acad. Sci. USA* **98**: 8270–8275.
- CASTAÑO, I. B., S. HEATH-PAGLIUSO, B. U. SADOFF, D. J. FITZHUGH and M. F. CHRISTMAN, 1996 A novel family of *TRF* (DNA topoisomerase I-related function) genes required for proper nuclear segregation. *Nucleic Acids Res.* **24**: 2404–2410.
- CIOSK, R., M. SHIRAYAMA, A. SHEVENKO, T. TANAKA, A. TOTH *et al.*, 2000 Cohesin's binding to chromosomes depends on a separate complex consisting of Scc2 and Scc4 proteins. *Mol. Cell* **5**: 243–254.
- DENG, J. Z., S. R. STARCK and S. M. HECHT, 1999 DNA polymerase beta inhibitors from *Baeckea gunniana*. *J. Nat. Prod.* **62**: 1624–1626.
- DUNN, B., and C. R. WOBBE, 1997 Preparation of protein extracts from yeast, pp. 13.13.1–13.13.9 in *Current Protocols in Molecular Biology*, edited by F. M. AUSUBEL, R. BRENT, R. E. KINGSTON, D. D. MOORE, J. G. SEIDMAN *et al.* John Wiley & Sons, New York.
- HANNA, J. S., E. S. KROLL, V. LUNDBLAD and F. A. SPENCER, 2001 *Saccharomyces cerevisiae* *CTF18* and *CTF4* are required for sister chromatid cohesion. *Mol. Cell. Biol.* **21**: 3144–3158.
- HOLMES, A. M., and J. E. HABER, 1999 Double-strand break repair in yeast requires both leading and lagging strand DNA polymerases. *Cell* **96**: 415–424.
- HSAING, Y. H., M. G. LIHOU and L. F. LIU, 1989 Arrest of replication forks by drug-stabilized topoisomerase I-DNA cleavable complexes as a mechanism of cell killing by camptothecin. *Cancer Res.* **49**: 5077–5082.
- HSU, H. Y., J. J. YANG and C. C. LIN, 1997 Effects of oleanolic acid and ursolic acid on inhibiting tumor growth and enhancing the recovery of hematopoietic system postirradiation in mice. *Cancer Lett.* **111**: 7–13.
- KABACK, D. B., P. W. OELLER, H. Y. DE STEENSMA, J. HIRSCHMAN, D. RUEZINSKY *et al.*, 1984 Temperature-sensitive lethal mutations on yeast chromosome I appear to define only a small number of genes. *Genetics* **108**: 67–90.
- LIU, L. F., 1989 DNA topoisomerase poisons as antitumor drugs. *Annu. Rev. Biochem.* **58**: 351–375.
- MICHAELIS, C., R. CIOSK and K. NASMYTH, 1997 Cohesins: chromosomal proteins that prevent premature separation of sister chromatids. *Cell* **91**: 35–45.
- NITISS, J. L., and J. C. WANG, 1996 Mechanisms of cell killing by drugs that trap covalent complexes between DNA topoisomerases and DNA. *Mol. Pharmacol.* **50**: 1095–1102.
- PELLETIER, H., M. R. SAWAYS, A. KUMAR, S. H. WILSON and J. KRAUT, 1994 Structures of ternary complexes of rat DNA polymerase beta, a DNA template-primer, and ddCTP. *Science* **264**: 1891–1903.
- SAWAYA, M. R., H. PELLETIER, A. KUMAR, S. H. WILSON and J. KRAUT, 1994 Crystal structure of rat DNA polymerase beta: evidence for a common polymerase mechanism. *Science* **264**: 1930–1935.
- SCHWARTZ, J. L., 1989 Monofunctional alkylating agent-induced S-phase dependent DNA damage. *Mutat. Res.* **16**: 111–118.
- SKIBBENS, R. V., L. B. CORSON, D. KOSHLAND and P. HIETER, 1999 Ctf7p is essential for sister chromatid cohesion and links mitotic chromosome structure to the DNA replication machinery. *Genes Dev.* **13**: 307–319.
- STRAIGHT, A. F., A. S. BELMONT, C. C. ROBINETT and A. W. MURRAY, 1996 GFP tagging of budding yeast chromosomes reveals that protein-protein interactions can mediate sister chromatid cohesion. *Curr. Biol.* **6**: 1599–1608.
- TAKAHASHI, K., and M. YANAGIDA, 2000 Cell cycle: replication meets cohesion (comment). *Science* **289**: 735–736.
- TERCERO, J. A., and J. F. X. DIFFLEY, 2001 Regulation of DNA replication fork progression through damaged DNA by the Mec1/Rad53 checkpoint. *Nature* **412**: 553–557.
- TOTH, A., R. CIOSK, F. UHLMANN, M. GALOVA, A. SCHLEIFFER *et al.*, 1999 Yeast cohesin complex requires a conserved protein, Eco1p(Ctf7), to establish cohesion between sister chromatids during DNA replication. *Genes Dev.* **13**: 320–333.
- UHLMANN, F., and K. NASMYTH, 1998 Cohesion between sister chromatids must be established during DNA replication. *Curr. Biol.* **8**: 1095–1101.
- WAGA, S., and B. STILLMAN, 1994 Anatomy of a DNA replication fork revealed by reconstitution of SV40 DNA replication *in vitro*. *Nature* **369**: 207–212.
- WALOWSKY, C., D. J. FITZHUGH, I. B. CASTAÑO, J. Y. JU, N. A. LEVIN *et al.*, 1999 The topoisomerase-related function gene *TRF4* affects cellular sensitivity to the antitumor agent camptothecin. *J. Biol. Chem.* **274**: 7302–7308.
- WANG, J., R. CHEN and D. A. JULIN, 2000 A single nuclease active site of the *Escherichia coli* RecBCD enzyme catalyzes single-stranded DNA degradation in both directions. *J. Biol. Chem.* **275**: 507–513.
- WANG, S. W., T. TODA, R. MACCALLUM, A. L. HARRIS and C. NORBURY, 2000 Cid1, a fission yeast protein required for S-M checkpoint control when DNA polymerase delta or epsilon is inactivated. *Mol. Cell. Biol.* **20**: 3234–3244.
- WANG, Z., I. B. CASTAÑO, A. DE LAS PEÑAS, C. ADAMS and M. F. CHRISTMAN, 2000 Pol kappa: a DNA polymerase required for sister chromatid cohesion. *Science* **289**: 774–779.
- WERTMAN, K. R., D. G. DRUBIN and D. BOTSTEIN, 1992 Systematic mutational analysis of the yeast *ACT1* gene. *Genetics* **132**: 33.
- XIAO, W., B. L. CHOW and L. RATHGEBER, 1996 The repair of DNA methylation damage in *Saccharomyces cerevisiae*. *Curr. Genet.* **30**: 461–468.

Communicating editor: M. LICHTEN